



Lawrence Berkeley Laboratory

UNIVERSITY OF CALIFORNIA

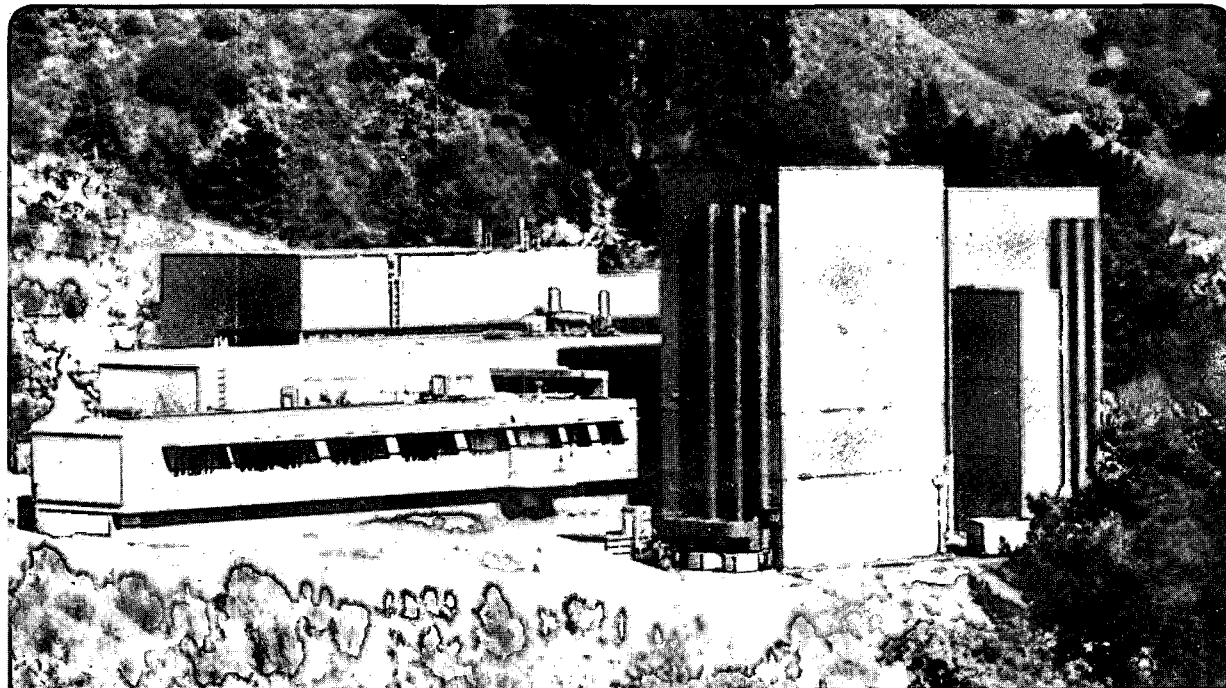
Materials & Chemical Sciences Division

National Center for Electron Microscopy

Atomic Structure of a $\Sigma 99$ Grain Boundary in Aluminum: A Comparison between Atomic-Resolution Observation and Pair Potential and Embedded Atom Simulations

U. Dahmen, C.J.D. Hetherington, M.A. O'Keefe, K.H. Westmacott,
M.J. Mills, M.S. Daw and V. Vitek

November 1989



Prepared for the U.S. Department of Energy under Contract Number DE-AC03-76SF00098.

LOAN COPY
Circulates
for 2 weeks

Bldg. 50 Library.
Copy 2

LBL-28123

DISCLAIMER

This document was prepared as an account of work sponsored by the United States Government. While this document is believed to contain correct information, neither the United States Government nor any agency thereof, nor the Regents of the University of California, nor any of their employees, makes any warranty, express or implied, or assumes any legal responsibility for the accuracy, completeness, or usefulness of any information, apparatus, product, or process disclosed, or represents that its use would not infringe privately owned rights. Reference herein to any specific commercial product, process, or service by its trade name, trademark, manufacturer, or otherwise, does not necessarily constitute or imply its endorsement, recommendation, or favoring by the United States Government or any agency thereof, or the Regents of the University of California. The views and opinions of authors expressed herein do not necessarily state or reflect those of the United States Government or any agency thereof or the Regents of the University of California.

Atomic Structure of a $\Sigma 99$ Grain Boundary in Aluminum: A Comparison
Between Atomic-Resolution Observation, Pair Potential and Embedded
Atom Simulations

U. Dahmen¹, C.J.D. Hetherington¹, M.A. O'Keefe¹, K.H. Westmacott¹, M.J. Mills², M.S.
Daw² and V. Vitek³

¹National Center for Electron Microscopy, Lawrence Berkeley Lab, Berkeley, Ca.
94720, ²Sandia National Labs, Livermore, Ca. 94551, ³Department of Materials Science,
University of Pennsylvania, Philadelphia, Pa. 19104

Abstract

An atomic resolution image of a symmetrical $\Sigma 99$ {557} <110> tilt boundary in aluminum is compared with images simulated from models based on atomistic calculations using pair potentials and the Embedded Atom Method. The two methods for atomistic modelling result in very similar structures, and image simulations based on such structures closely match the experimental results.

Recent improvements in the resolution limit of transmission electron microscopes to below 0.2 nm allow direct imaging of the atomic structure of grain boundaries in close packed metals and detailed comparison with theoretical predictions. This letter describes such a study for a $\Sigma 99$ grain boundary in aluminum.

Continuous bicrystals of aluminum deposited on $\langle 100 \rangle$ silicon substrates exhibit grain boundary facets on $\{557\}$ crystallographic planes with a disorientation between grains of nearly 90° about a $\langle 110 \rangle$ axis [1,2,3]. The crystallographic description specifies these as $\Sigma 99$ $(557)/(55\bar{7})$ 89.4° $[1\bar{1}0]$ symmetrical tilt boundaries. An atomic resolution micrograph of a short segment of such a boundary was taken on the JEOL ARM 1000 at an accelerating voltage of 800 kV and a defocus of -80 nm in a region of a foil not exceeding about 12 nm in thickness. Under these imaging conditions the atomic columns (which were accurately parallel to the electron beam) appeared as white dots and atomic relaxation of the crystal lattice at the boundary into structural units [4] was clearly visible.

For comparison with the experimental image, image simulations were conducted for relaxed boundary structures modelled atomistically. The same boundary was studied theoretically with two atomistic approaches: pair potential (PP) and embedded atom method (EAM). The pair potential used was developed by Dagens et al. [5] from a jellium reference state at the electronic density of bulk aluminum. In that work, the interatomic potentials were obtained by calculating the perturbation to second order in the ionic pseudopotential. The pair potential for aluminum is such that both the first and second nearest neighbor are on its repulsive side [6]. This potential form leads to a behavior close to that of hard spheres and an aluminum lattice that is very rigid up to the boundary, allowing only small relaxations. This has been confirmed in previous studies of relative displacements of annealing twins in aluminum which were found to be close to those determined on a hard sphere model [7].

The EAM, by comparison, does not incorporate Fermi surface effects or exact screening, but does a more careful accounting of coordination effects and is explicitly a many-body potential [8]. The effective pair potential [9] which can be derived from the empirical EAM potential used in these calculations [10] is such that the first and second neighbors are positioned on the repulsive and attractive parts of this potential, respectively. This form of the potential leads to larger flexibility of the structure.

Both computational methods proceeded by starting with various geometrically determined candidate structures and carrying out full energy minimizations. Several different relaxed structures were thereby produced. Multiplicity of grain boundary structures is a common phenomenon [11] but through an iterative comparison with the experimental image inadequate matches with several PP structures were eliminated and the best match readily identified. This structure was very similar to the minimum energy structure determined by EAM. In addition to static energy minimization this lowest energy structure was annealed in Monte Carlo simulations with the EAM at 800K with no change, indicating that it was indeed the lowest-energy, stable configuration.

The EAM calculated boundary structure shown in Fig. 1a is clearly less 'open' than the PP structure in Fig. 1b, in which well-defined tunnels between the atoms are easily identified. This is shown quantitatively in Fig. 1c where the arrows centered at atomic positions show the difference between atomic displacements in EAM and PP structures. Clearly, this difference is largest (about 0.05 nm) for the two atoms surrounding the characteristic pair that gives rise to the strong contrast in the high resolution image (see Fig. 2b). Relaxation of these two atoms determines the openness of the tunnels in the structure. In addition, the relative displacement across the boundary plane is slightly different for the two structures. As seen in fig.

1c this displacement has a component parallel to the boundary plane of about 0.01 nm.

Image simulations [12] based on the two calculated structure models described above are compared with the experimental image in fig. 2. To reduce the effect of noise the image was averaged over five half-periods of the boundary, see fig. 2b. Only two half-periods (identical in projection) are shown. Each structural unit has a characteristic appearance of two well-separated strong white dots (marked) on the boundary plane surrounded by several partially-connected weaker dots. In addition, a lattice relaxation is apparent within a few atomic distances of the boundary. A rigid body displacement parallel to the boundary was measured to be 0.05 ± 0.01 nm. Since the foil thickness was not known with accuracy, images were simulated for a range of realistic foil thicknesses in 0.56 nm increments. The best match for each model was determined visually by comparing the characteristic intensity in the boundary plane with that in the experimental image. Good matches were found for a thickness of 4.6 nm for the EAM (fig. 2a) and 10.3 nm for the PP structure (fig. 2c). The small black dots overlaid on the two simulated images marking atomic positions illustrate that not all white dots in an image correspond to projected atom positions since some white dots appear at positions of tunnels in the boundary. Image simulations are therefore always necessary before a micrograph of a defect structure such as that shown here can be fully interpreted.

Each half-period of the experimental image (fig. 2b) exhibits the characteristic pair of strong white dots aligned parallel to the boundary plane, framed by several white spots of lower intensity. Halfway between the two pairs of dots on the boundary there is a region of relatively perfect crystal. In this region the agreement between the experimental and calculated images is best. As seen in the arrow plot of relative displacements in fig. 1c this is also the region where the two models agree most

closely. It is in the boundary regions immediately surrounding the pair that the two models differ most noticeably from each other and from the image. First, the pair in the experimental image has stronger contrast than its counterpart in the simulated images. In addition, both models show these spots aligned at a small angle to the plane of the boundary rather than parallel as in the image.

To make this comparison more quantitative, a direct overlay of the simulated and experimental images is shown in figs 2d and f. To produce these composite figures the simulated images of the two models (fig 2a and c) were reversed contrast (small black dots) and superimposed on the experimental image (large white dots). In the overlaid black spot images the contrast level was enhanced in order to produce a smaller spot size which leaves the experimental white spot image visible. To assess the validity of this procedure, fig 2e shows an overlay of the experimental image on itself, using the same method of contrast reversal and enhancement. It is apparent from this figure that the black regions (relatively large due to saturation of the emulsion) of the enhanced image appear centered on the intensities of the white image. Hence a shift of a black intensity in figs 2d and f signifies a difference in atom positions.

The positions of the image intensities are seen to be very closely matched in both these overlays. In the PP structure (Fig. 2f) these connected intensities are generally in the same locations and have the same shape as in the observed image. However, they are missing immediately below the characteristic pair of spots where weakly linked intensity is found in the experimental image. On the other hand, in the EAM structure (Fig. 2d), the two most pronounced connected intensities are in the same positions as in the PP structure, but their shapes are different. Furthermore, in the location below and to the right of the characteristic pair, a streaked intensity is simulated that is not present in the observed image. A more detailed interpretation of

the connected intensities is not attempted here because of uncertainties in experimental parameters such as the thicknesses of the foil and the contamination layer, and the lack of a through-focus series of images.

Despite the subtle differences described above, the match between the experimental and calculated images is good for both calculated structures. Because it was possible to discard unambiguously a number of other structures found in the process of computer modeling as clearly mismatched with the observation, a comparison of this kind is an accurate measure of the quality of the match between theory and experiment. This is an important point since it demonstrates that the technique of high resolution microscopy now allows the experimental distinction between different atomic boundary structures in close packed metals. However, the structures calculated by the two theoretical approaches were so similar that it was not possible within the experimental limitations at this time to decide which describes the observed structure more closely. The fact that in a short facet of such a high- Σ bicrystal the two models appear to converge on the same structure as that observed is an encouraging result. A full account of this work will be published elsewhere.

Acknowledgements

We thank J. Turner for assistance with the image processing, I. Yamada for providing the ICB Al sample and J.-M. Penisson for helpful discussions. This work was supported by the Director, Office of Energy Research, Office of Basic Energy Sciences of the U.S. Department of Energy under contracts #DE-AC03-76SF00098 (UD, CJDH, MAOK, KHW) and #DE-AC04-76DP00789 (MM, MD) and by the National Science Foundation, MRL Program DMR88-19885 (VV).

References

1. T. Takagi, I. Yamada and A. Sasaki, J. Vac. Sci. Technol. A2, 382 (1984)

- 2 U. Dahmen and K.H. Westmacott, *Scr. Met.* 22, 1673 (1988)
- 3 M.C. Madden, *Appl. Phys. Lett.* 55, 1077 (1989)
- 4 A.P. Sutton and V.Vitek, *Phil. Trans. Roy. Soc. London A* 309, 1 (1983)
- 5 L. Dagens, M. Rasolt and R. Taylor, *Phys. Rev. B* 11, 2726 (1975)
- 6 V. Vitek and M. Minonishi, *Surf. Sci.* 144, 196 (1984)
- 7 R.C. Pond and V. Vitek, *Proc. Roy. Soc. A* 357, 453 (1977)
- 8 M.S. Daw and M.I. Baskes, *Phys. Rev. Lett.* 50, 1285 (1983)
and *Phys. Rev. B* 29, 6443 (1984)
- 9 S.M. Foiles, *Phys. Rev. B* 32, 3409 (1985)
- 10 A.F. Voter and S.P. Chen, *MRS Proc.* 82, 175 (1987)
- 11 G.J. Wang, V. Vitek and A.P. Sutton, *Acta Met.* 32, 1093 (1984)
- 12 M.A. O'Keefe, P.R. Buseck and S. Iijima, *Nature* 274, 322 (1978)

Figure Captions

Fig. 1 Comparison of the lowest energy structures calculated by the two computational models, EAM (a) and PP (b). The displacement map (c) compares the two simulated structures by arrows (not to scale) pointing from EAM to PP. The longest arrow corresponds to a relative atomic displacement of about 0.05 nm.

Fig. 2 Comparison of images simulated from (a) the EAM and (c) the PP structure with the averaged experimental image (b). Superposition of the images shown in (a)-(c) in reversed and enhanced contrast over the experimental image illustrates the match for the EAM (d) and PP (f). This type of comparison is validated by (e) where the image in reversed and enhanced contrast is overlaid on itself (although note that due to the response of the photographic emulsion the black spots are larger than in the neighboring images).

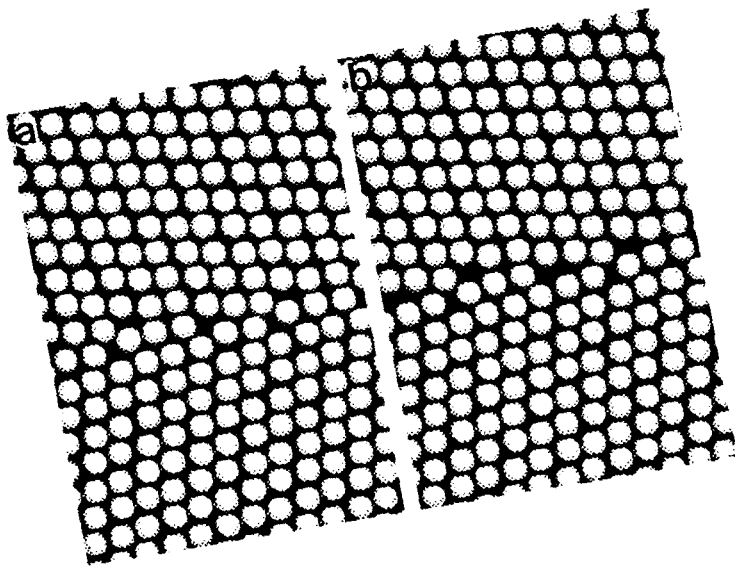


Figure 1, a,b

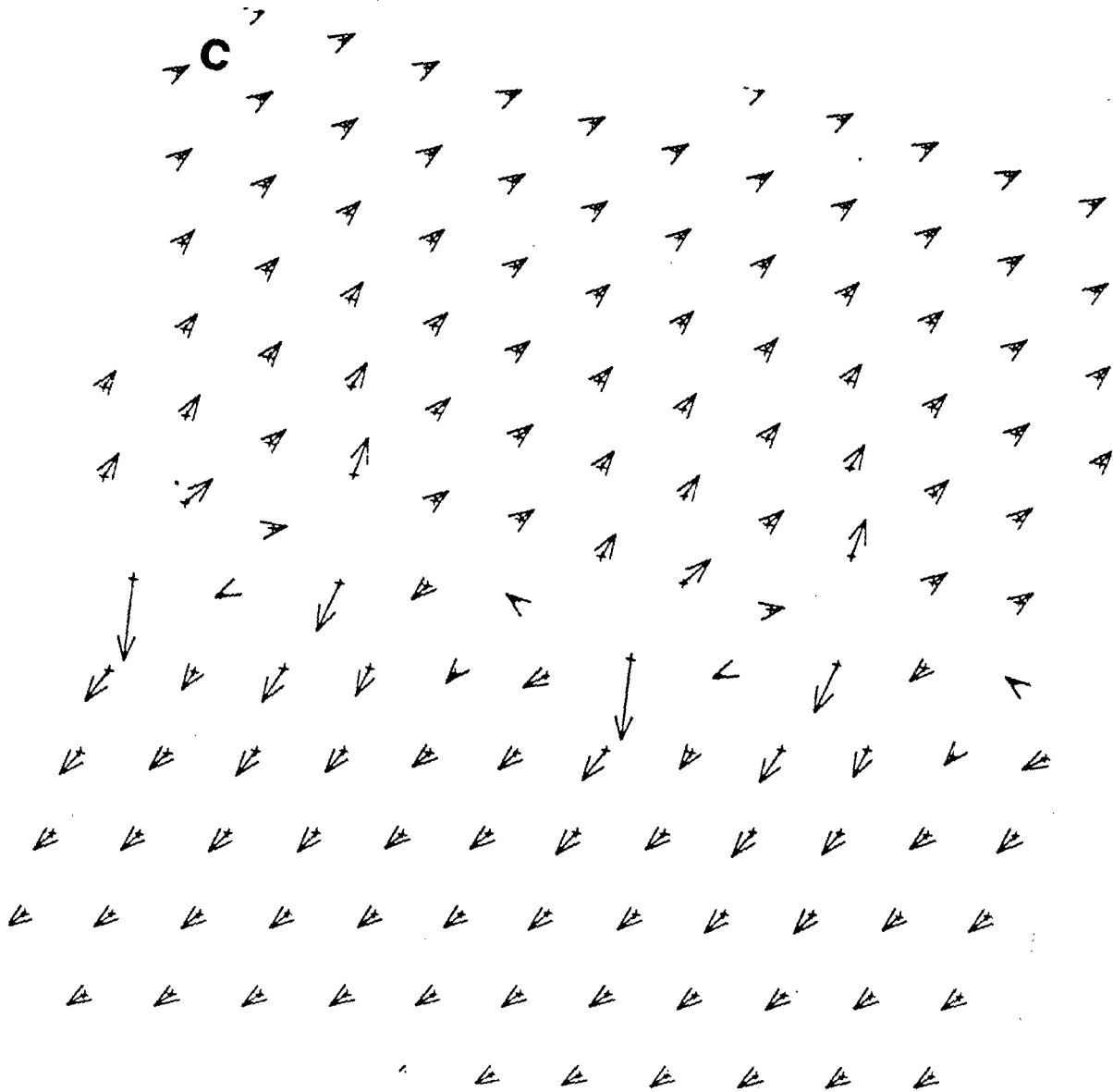


Figure 1c

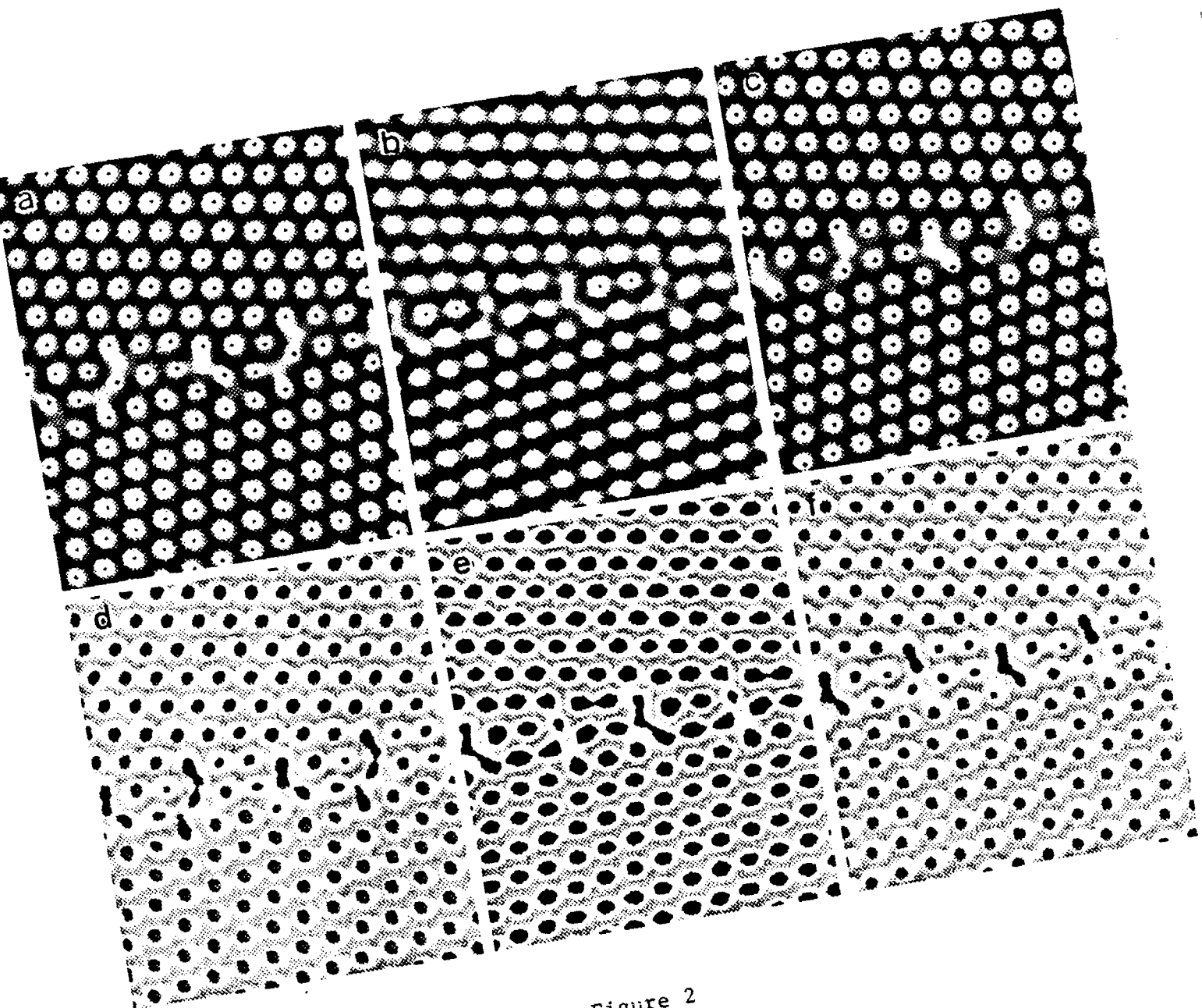


Figure 2

LAWRENCE BERKELEY LABORATORY
TECHNICAL INFORMATION DEPARTMENT
1 CYCLOTRON ROAD
BERKELEY, CALIFORNIA 94720